Synthesis of Dual-Band Bandpass Filters Using Successive Frequency Transformations and Circuit Conversions

Xuehui Guan, Zhewang Ma, Peng Cai, Yoshio Kobayashi, Tetsuo Anada, and Gen Hagiwara

***Abstract*—A novel method is proposed to synthesize dual-band bandpass filters (BPFs) from a prototype low-pass filter. By implementing successive frequency transformations and circuit conversions, a new filter topology is obtained which consists of only admittance inverters and series resonators, and is thereby easy to be realized by using conventional distributed elements. A dual-band BPF with center frequencies of 1.8 GHz and 2.4 GHz is designed and fabricated using microstrip lines and stubs. The simulated and measured results show a good agreement and validate the proposed theory.**

***Index Terms*—Admittance inverter, dual-band filter, frequency transformation, microstrip line.**

I. Introduction

RAPID development of modern communications demands efficient utilization of more and more frequency channels. To reduce the volume and weight of communication circuits and equipment, many dual-band and multiband components, including antennas [1], amplifiers [2], and microwave filters [3]–[5] have been developed. A number of publications have provided a variety of solutions to the realization of dual-band bandpass filters (BPFs). Miyake *et al.* [3] used two different parallel-connected filters to obtain dual-band characteristics. Tsai and Hsue [4] inserted a stopband into a broadband to form dual-bands by cascading a broadband BPF with a narrowband bandstop filter. Because the circuit configurations in both [3] and [4] include two different filters, the sizes of these dual-band filters are comparatively large. Recently, Chang *et al.* reported dual-band BPFs employing stepped impedance resonators (SIRs) [5]. One of the advantages of the SIR filter is that the positions of the dual-bands can be designed conveniently. However, it confronts difficulties when making adjustment of coupling coefficients between neighboring resonators to meet, simultaneously, the dual bandwidth specifications of the filter.

Manuscript received August 2, 2005; revised November 29, 2005. This work was supported in part by the National Natural Science Foundation of China (GP60271029) and the High-Tech Research Center Project from the Ministry of Education, Culture, Sports, Science, and Technology, Japan.

X. Guan and P. Cai are with the School of Communication and Information Engineering, Shanghai University, Shanghai 200072, China (e-mail: xuehuiguan@yahoo.com.cn).

Z. Ma and Y. Kobayashi are with the Department of Electrical and Electronic Systems, Saitama University, Saitama 338-8570, Japan (e-mail: ma@ees.saitama-u.ac.jp).

T. Anada is with the High-Tech Research Center, Kanagawa University, Kanagawa 52-8520, Japan.

G. Hagiwara is with Link Circuit, Inc., Kawaguchi City 333-0844, Japan.

Digital Object Identifier 10.1109/LMWC.2006.869868

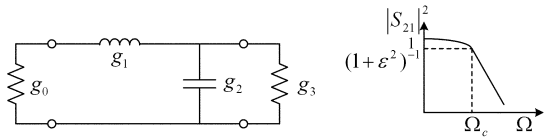

Fig. 1. Two-pole prototype LPF and its transmission characteristics.

Uchida *et al.* [6] developed a dual-band-rejection filter with smaller passband insertion loss through the formation of two closely spaced rejection bands, using a novel frequency-transformation. In this letter, the frequency-transformation technique is extended to develop a new synthesis theory for the design of dual-band BPFs. The theory commences with a conventional prototype low-pass filter (LPF) and a frequency transformation, which converts the prototype LPF into a BPF. After a second frequency transformation is carried out, the BPF is converted into a dual-band BPF. The dual-band BPF has a complicated configuration compared with those of conventional BPFs. To simplify the realization of the obtained dual-band BPF using distributed transmission lines or waveguides, admittance inverters are introduced successively to evolve the filter into new topologies. The final circuitry of the dual-band filter consists of only series LC resonators and admittance inverters, and hence can be easily realized by using distributed transmission lines and conventional design techniques. To verify the proposed theory, a dual-band BPF operating at 1.8 GHz and 2.4 GHz is designed and fabricated in a microstrip form. It is found that the measured response of the filter agrees well with the simulated result.

II. Synthesis Theory

Fig. 1 shows a two-pole prototype LPF and its schematic transmission characteristics. The element values of g_0, g_1, g_2, and g_3 in the prototype filter are determined by its passband specifications using the well-known formulas in [7], and ε is a constant relating to the maximum insertion loss in the passband.

The prototype LPF is converted to a BPF by executing the following frequency transformation [7]:

$$\Omega = \frac{\Omega_c}{\mathrm{FBW}_0}\left(\frac{\omega'}{\omega_0} - \frac{\omega_0}{\omega'}\right) \tag{1}$$

where Ω and ω' are angular frequencies of the LPF and BPF, respectively, $\Omega_c = 1$ rad/s is the cutoff angular frequency of the prototype LPF, FBW_0 and ω_0 are the fractional bandwidth and center frequency of the BPF, respectively. Through this transformation, the series inductor and shunt capacitor in the LPF are

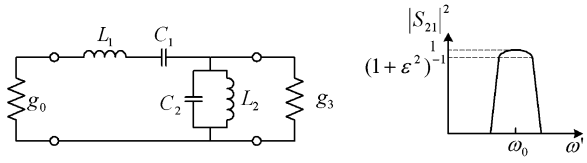

Fig. 2. Two-pole BPF and its transmission characteristics.

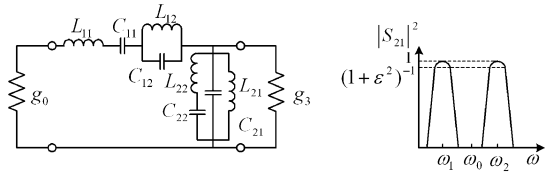

Fig. 3. Two-pole dual-band BPF and its transmission characteristics.

converted to a series and a shunt LC resonator, respectively, in the BPF shown in Fig. 2. The schematic transmission response of the BPF is also given in Fig. 2. The expressions for the circuit elements in Fig. 2 are as follows:

$$L_1 = \frac{g_1\Omega_c}{\mathrm{FBW}_0\omega_0}, \quad C_1 = \frac{1}{L_1\omega_0^2} \tag{2}$$

$$L_2 = \frac{\mathrm{FBW}_0}{g_2\Omega_c\omega_0}, \quad C_2 = \frac{1}{L_2\omega_0^2}. \tag{3}$$

The BPF is further converted to a dual-band BPF when the following frequency transformation [6] is conducted:

$$\omega' = \frac{\omega_0}{\mathrm{FBW}}\left(\frac{\omega}{\omega_0} - \frac{\omega_0}{\omega}\right) \tag{4}$$

where ω is the angular frequency of the dual-band BPF, ω_1 and ω_2 are the center angular frequencies of the first and second passband of the dual-band filter, $\mathrm{FBW} = (\omega_2 - \omega_1)/\omega_0$, and $\omega_0 = (\omega_1\omega_2)^{1/2}$.

In the case of a narrow band (FBW_1 <0.1) filter, we get

$$\mathrm{FBW}_1 = \mathrm{FBW}_2 = \mathrm{FBW}_0\frac{\omega_2 - \omega_1}{\omega_1 + \omega_2} \tag{5}$$

here FBW_1 and FBW_2 are the fractional bandwidths of the first and second passband of the dual-band filter, respectively. The circuit configuration of the obtained two-pole dual-band BPF is shown in Fig. 3, where the schematic transmission characteristics of the filter are also depicted. Through a little bit tedious but straightforward formulation, we get the expressions for the circuit elements in Fig. 3 as follows:

$$L_{11} = \frac{g_1\Omega_c}{\mathrm{FBW}_0(\omega_2 - \omega_1)}, \quad C_{11} = \frac{1}{L_{11}\omega_0^2} \tag{6}$$

$$L_{12} = \frac{g_1\Omega_c(\omega_2 - \omega_1)}{\mathrm{FBW}_0\omega_0^2}, \quad C_{12} = \frac{1}{L_{12}\omega_0^2} \tag{7}$$

$$L_{21} = \frac{\mathrm{FBW}_0(\omega_2 - \omega_1)}{g_2\Omega_c\omega_0^2}, \quad C_{21} = \frac{1}{L_{21}\omega_0^2} \tag{8}$$

$$L_{22} = \frac{\mathrm{FBW}_0}{g_2\Omega_c(\omega_2 - \omega_1)}, \quad C_{22} = \frac{1}{L_{22}\omega_0^2}. \tag{9}$$

It is observed that the circuit configuration of the dual-band BPF in Fig. 3 becomes fairly complicated compared with that of the conventional BPF in Fig. 2. Its series and shunt branches

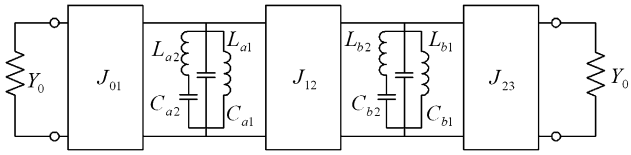

Fig. 4. Dual-band BPF with J-inverters, series and shunt LC resonators.

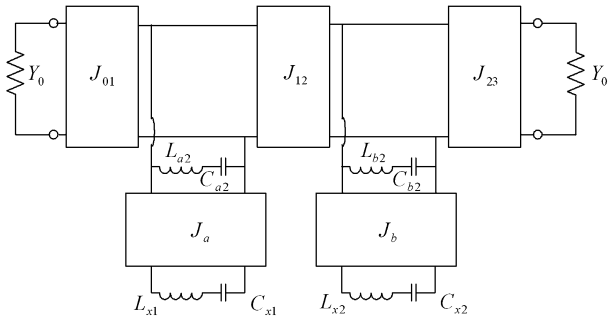

Fig. 5. Dual-band BPF with only J-inverters and series LC resonators.

now include both series and shunt LC resonators. Such a circuit is difficult to realize at microwave frequencies when using distributed transmission lines. Therefore, successive circuit conversions are implemented below. First, the series branch is replaced by a shunt branch with the aid of admittance inverters (J-inverters), as shown in Fig. 4. Circuit elements in Fig. 4 are determined by the following expressions:

$$L_{ai} = \frac{g_0Y_0}{J_{01}^2}C_{1i}, \quad L_{bi} = \frac{J_{01}^2}{g_0Y_0J_{12}^2}L_{2i}, \quad i = 1,2 \tag{10}$$

$$L_{a1}C_{a1} = L_{a2}C_{a2} = L_{b1}C_{b1} = L_{b2}C_{b2} = \frac{1}{\omega_0^2} \tag{11}$$

$$J_{12} = \frac{J_{01}J_{23}}{Y_0}\sqrt{\frac{g_3}{g_0}}. \tag{12}$$

Although the circuit in Fig. 4 contains only shunt branches now, each of the shunt branches includes both series and shunt LC resonators. Therefore, a further step of circuit conversion is implemented by replacing all the shunt resonators with series resonators through the assistance of admittance inverters. The obtained filter is shown in Fig. 5, which consists of J-inverters and series LC resonators only. The derived formulas for the circuit elements in Fig. 5 are given as

$$J_a = J_{01}\sqrt{\frac{C_{x1}}{g_0Y_0C_{11}}}, \quad J_b = J_{23}\sqrt{\frac{g_3C_{x2}}{Y_0L_{21}}}$$

$$J_{12} = \frac{J_{01}J_{23}}{Y_0}\sqrt{\frac{g_3}{g_0}} \tag{13}$$

$$L_{x1}C_{x1} = L_{x2}C_{x2} = \frac{1}{\omega_0^2}. \tag{14}$$

As shown in (13) and (14), the elements C_{x1}, C_{x2}, J_{01}, and J_{23} may take arbitrary values. However, in practice, their values need to be chosen appropriately so that physical dimensions of these elements can be realized without much difficulty. The admittance inverters, J_a, J_b, and J_{12} are then determined by using (13). The flexibility in choosing the parameters allows us more freedom in the design and realization of dual-band BPFs.

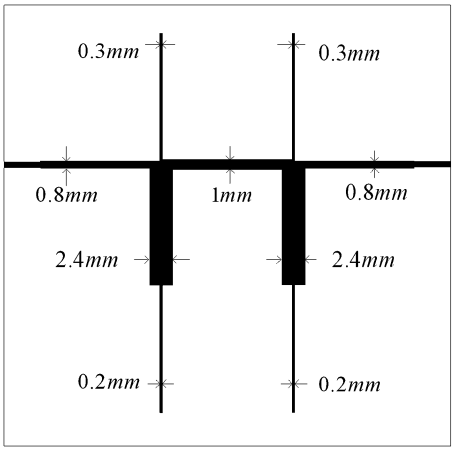

Fig. 6. Microstrip realization of a dual-band BPF.

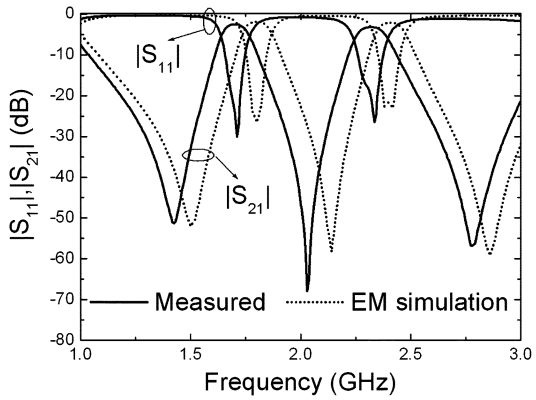

Fig. 7. Simulated and measured responses of the fabricated dual-band filter.

III. Design Example

A dual-band Chebyshev BPF, based on the topology in Fig. 5, is designed using microstrip lines to validate the theory proposed above. The central frequencies of the dual-bands are 1.8 and 2.4 GHz, respectively. The ripple in the passbands is 0.01 dB, and the equal-ripple bandwidth of both the first and second passband is 2.78%, i.e., 50 and 67 MHz, respectively. The admittance inverters in Fig. 5 are realized by employing microstrip quarter-wavelength lines, while the series LC resonator are realized by using microstrip quarter-wavelength open stubs [8].

Fig. 6 shows the configuration and dimensions of our designed dual-band filter, using the commercial substrate Duriod 6010 with a relative dielectric constant of 10.2, a loss tangent of 0.0023, and a thickness of 0.635 mm. The stubs in Fig. 6 with width 0.8, 1.0, and 2.4 mm are quarter-wavelength admittance inverters, and the remaining four open stubs are four series LC resonators.

Fig. 7 provides a comparison of the simulated and measured characteristics of the filter. The solid lines are measured response of the fabricated filter, using a network analyzer HP8722ES. The dashed lines are simulated curves of the microstrip filter shown in Fig. 7, using a full-wave electromagnetic solver [9]. Both the dielectric and conductor (with a conductivity of $\sigma = 5.8 \times 10^7$ S/m of copper) loss are taken into account in the simulation. The agreement over the dual bands is good with the exception of a frequency shift which occurs between the simulated and measured responses. Such a frequency shift is observed in most previous reports of filters, and is mainly caused by the deviation of dielectric constant between the nominal and its real values, and by the fabrication tolerance of the filter. A transmission zero at about 2.1 GHz is clearly observed, which produces sharp and large attenuations between the dual passbands of the filter.

IV. Conclusion

A new synthesis method of dual-band microwave BPFs is proposed. By implementing two successive frequency transformations, a dual-band BPF is obtained from a prototype LPF. A new topology of dual-band BPF is obtained, and its realization is made easy by carrying out circuit conversions using admittance inverters. The design example in a microstrip form provides a good agreement between the measured and simulated frequency response of the filter and verifies thereby the proposed theory. Although the theory and example is described for a second order filter, its extension to higher order filters is straightforward and follows the same procedure described in Section II.

References

[1] Y. L. Kuo and K. L. Wong, "Printed double-T monopole antenna for 2.4/5.2 GHz dual-band WLAN operations," *IEEE Trans. Antennas Propag.*, vol. 51, no. 9, pp. 2187–2192, Sep. 2003.

[2] H. Hashemi and A. Hajimiri, "Concurrent multiband low-noise amplifiers theory, design and applications," *IEEE Trans. Microw. Theory Tech.*, vol. 50, no. 1, pp. 288–301, Jan. 2002.

[3] H. Miyake, S. Kitazawa, T. Ishizaki, T. Yamada, and Y. Nagatomi, "A miniaturized monolithic dual band filter using ceramic lamination technique for dual mode portable telephones," in *IEEE MTT-S Int. Dig.*, 1997, pp. 789–792.

[4] L. C. Tsai and C. W. Hsue, "Dual-band bandpass filters using equal-length coupled serial-shunted lines and Z-transform technique," *IEEE Trans. Microw. Theory Tech.*, vol. 52, no. 4, pp. 1111–1117, Apr. 2004.

[5] S. F. Chang, Y. H. Jeng, and J. L. Chen, "Dual-band step-impedance bandpass filter for multimode wireless LANs," *Electron. Lett.*, vol. 40, pp. 38–39, Jan. 2004.

[6] H. Uchida, H. Kamino, K. Totani, N. Yoneda, M. Miyazaki, Y. Konishi, S. Makino, J. hirokawa, and M. Ando, "Dual-band-rejection filter for distortion reduction in RF transmitters," *IEEE Trans. Microw. Theory Tech.*, vol. 52, no. 11, pp. 2550–2556, Nov. 2004.

[7] G. Matthaei, L. Young, and E. M. T. Jones, *Microwave Filter, Impedance- Matching Networks, and Coupling Structures*. Norwood, MA: Artech House, 1980.

[8] Z. Ma and Y. Kobayashi, "Design and realization of bandpass filters using composite resonators to obtain transmission zeros," in *Proc. 35th Eur. Microw. Conf.*, Oct. 2005, pp. 1255–1258.

[9] *Sonnet suite*, Sonnet Software, Inc., Liverpool, NY, 2004.